

A novel *AGGF1-PDGFRβ* fusion in pediatric T-cell acute lymphoblastic leukemia

With contemporary multiagent chemotherapy regimens, event-free survival rates for children with T-cell acute lymphoblastic leukemia (T-ALL) exceed 85%, paralleling those observed in B-lineage acute lymphoblastic leukemia (B-ALL).¹ Outcomes for patients with relapsed and refractory T-ALL remain dismal.² In contrast to B-ALL, the prognostic relevance of blast karyotype has not been well established for pediatric T-ALL and has limited impact on treatment approaches. We report a case of refractory T-ALL harboring a novel fusion of platelet-derived growth factor receptor β (*PDGFRβ*).

A 4-year old boy presented with a 1-week history of fatigue, weakness, fever and vomiting. His physical examination was notable for prominent hepatosplenomegaly and his initial complete blood count showed a white blood cell count of $622.8 \times 10^9/L$ with 88% blasts, a platelet count of $71 \times 10^9/L$ and hemoglobin of 9.7 g/dL. A diagnostic bone marrow aspirate showed 90% T lymphoblasts and cerebrospinal fluid evaluation revealed leukemic involvement. The blast population expressed CD2, cytoplasmic CD3, CD5, CD7, CD8, CD34 (partial), CD38, and cTdT and lacked CD1a, surface CD3, CD4, HLA-Dr, cMPO, T-cell receptor $\alpha\beta$ or $\gamma\delta$. Cytogenetic studies on the diagnostic bone marrow aspirate showed added material of uncertain origin on chromosomes 3 and 5 (46,XY,add(3)(q21),add(5)(q11)[9]/46,XY[11]). Fluorescence *in situ* hybridization (FISH) testing for *BCR-ABL1* was negative. Induction therapy was initiated with vincristine, dexamethasone, pegaspargase, daunorubicin and intrathecal methotrexate. After an initial clinical response, the patient developed progressive disease with a rising absolute blast count and worsening splenomegaly on day 22. Augmented Berlin-Frankfurt-Münster consolidation therapy was initiated, with symptomatic improvement. Persistent disease was still evident after an additional month of treatment (16.3% marrow blasts) and salvage chemotherapy was initiated (Figure 1A, *Online Supplementary Table S1*).

Subsequently, targeted RNA sequencing (FoundationOne) identified a fusion of angiogenic factor with G patch and FHA domains 1 (*AGGF1*; 5q13.3) with *PDGFRβ* (5q33.1), which was confirmed by sequencing of the entire coding region (Figure 1B; *Online Supplementary Table S2*). Variants of unknown significance were detected in *ATR*, *CCND1*, and *SMARCA4*; no *NOTCH1* alterations were detected. The exact position of the *AGGF1-PDGFRβ* fusion was independently established from RNASeq data (day 75 specimen) using JAFFA and ChimeraScan fusion transcript detection algorithms (*Online Supplementary Figure S1*). Interphase FISH on peripheral blood verified a *PDGFRβ* (5q33.1) rearrangement in 71.5% of cells (Figure 1C) with a white blood cell count of $3.9 \times 10^9/L$ and 66% blasts by morphology. G-banding showed the same derivative chromosome 3 and 5 abnormalities as at diagnosis (*Online Supplementary Figure S2A*). Single nucleotide polymorphism microarray analysis of tumor DNA showed a 4.6 megabase (Mb) 5q14.1-14.2 deletion, a 405-kilobase (kb) 3q21.1 deletion, a 169-kb 9p21.3 deletion involving *CDKN2A*, a recurrent abnormality in T-ALL, and a 2.5-kb deletion involving exons 9 and 10 of *PDGFRβ* (*Online Supplementary Figure S2B-E*). Figure 1B shows a schematic of the chromosomal inversion, which is supported by several different findings. Importantly, RNA sequencing demonstrated an *AGGF1-PDGFRβ* fusion gene, which

requires inversion since the genes are normally transcribed in opposite directions. Second, the single nucleotide polymorphism array demonstrated a 5q14.1-14.2 deletion and a probable 2.5 kb deletion involving exons 9 and 10 of *PDGFRβ*, consistent with the break-points of the chromosomal inversion and the identified fusion protein that starts at exon 11 of *PDGFRβ*. Finally, metaphase FISH analysis with *PDGFRβ* probes was consistent with a paracentric inversion of chromosome 5. Qualitative reverse transcriptase polymerase chain reaction for the *AGGF1-PDGFRβ* fusion confirmed its presence in diagnostic and longitudinal (day 114) specimens (Figure 1A,D).

The in-frame fusion transcript encodes an 1124-residue protein: the N-terminal 544 residues (exons 1-10) of *AGGF1*, an alanine encoded by one *AGGF1* and two *PDGFRβ* nucleotides, and the C-terminal 579 residues (exons 11-23) of *PDGFRβ* (Figure 1E). The N-terminal region of *AGGF1* contains a coiled-coil dimerization domain, likely to promote constitutive autoactivation of the kinase component. No mutations were detected within the coding sequence of *AGGF1-PDGFRβ* at diagnosis or in serial specimens.

Constitutively activated *PDGFRβ* is observed in a variety of malignancies and can be inhibited with several approved tyrosine kinase inhibitors. Fresh bone marrow mononuclear cells collected at a point of persistent disease (day 114)(Figure 1A) with 76% blasts were subjected to *ex vivo* sensitivity profiling with a panel of kinase inhibitors approved by the Food and Drug Administration or in clinical development.³ A striking signature of response to tyrosine kinase inhibitors with target profiles that include *PDGFRβ* was evident (Figure 2A), including dasatinib (*ex vivo* IC₅₀: 2.2 nM)(Figure 2B). The dose-response curve for dasatinib leveled off before reaching zero, and this was observed to varying degrees for each of the effective tyrosine kinase inhibitors. This pattern could reflect the presence of 24% non-blast cells in the assay culture or a tyrosine kinase inhibitor-resistant blast subpopulation. Serial FISH and cytogenetic determinations conducted prior to dasatinib treatment (71.5% *AGGF1-PDGFRβ* positive), near the end of effective dasatinib therapy (19.5% *AGGF1-PDGFRβ* positive) and at progression (8.0% *AGGF1-PDGFRβ* positive) exhibited a pattern of declining *AGGF1-PDGFRβ* positivity (*Online Supplementary Table S3*), suggesting that an *AGGF1-PDGFRβ*-negative blast subpopulation is selected under dasatinib therapy. These FISH findings were supported by routine cytogenetic testing, which also showed a decline in the population with abnormalities in 5q over time after dasatinib was initiated (*Online Supplementary Table S3*).

To establish whether *AGGF1-PDGFRβ* is a transforming fusion kinase, *AGGF1-PDGFRβ* was cloned into the pMSCV-IRES-GFP (pMIG) expression vector, Ba/F3 cells were retrovirally transduced and interleukin-3 was withdrawn. Ba/F3 *AGGF1-PDGFRβ* cells proliferated in the absence of interleukin-3; Ba/F3 cells did not (Figure 2C; *Online Supplementary Figure S3*). Results from profiling of Ba/F3 *AGGF1-PDGFRβ* cells against a panel of clinically relevant *PDGFRβ* inhibitors, including dasatinib, were consistent with *ex vivo* sensitivities, supporting the role of constitutively activated *PDGFRβ* kinase in driving proliferation (Figure 2D). Immunoblot analysis confirmed the presence of *AGGF1-PDGFRβ* as an *AGGF1*- and *PDGFRβ*-immunoreactive band not present in Ba/F3 cells (Figure 2E). Analogous immunoblot experiments with flow-sorted blasts from a peripheral blood specimen (day 75) confirmed the presence of *AGGF1-PDGFRβ* (Figure

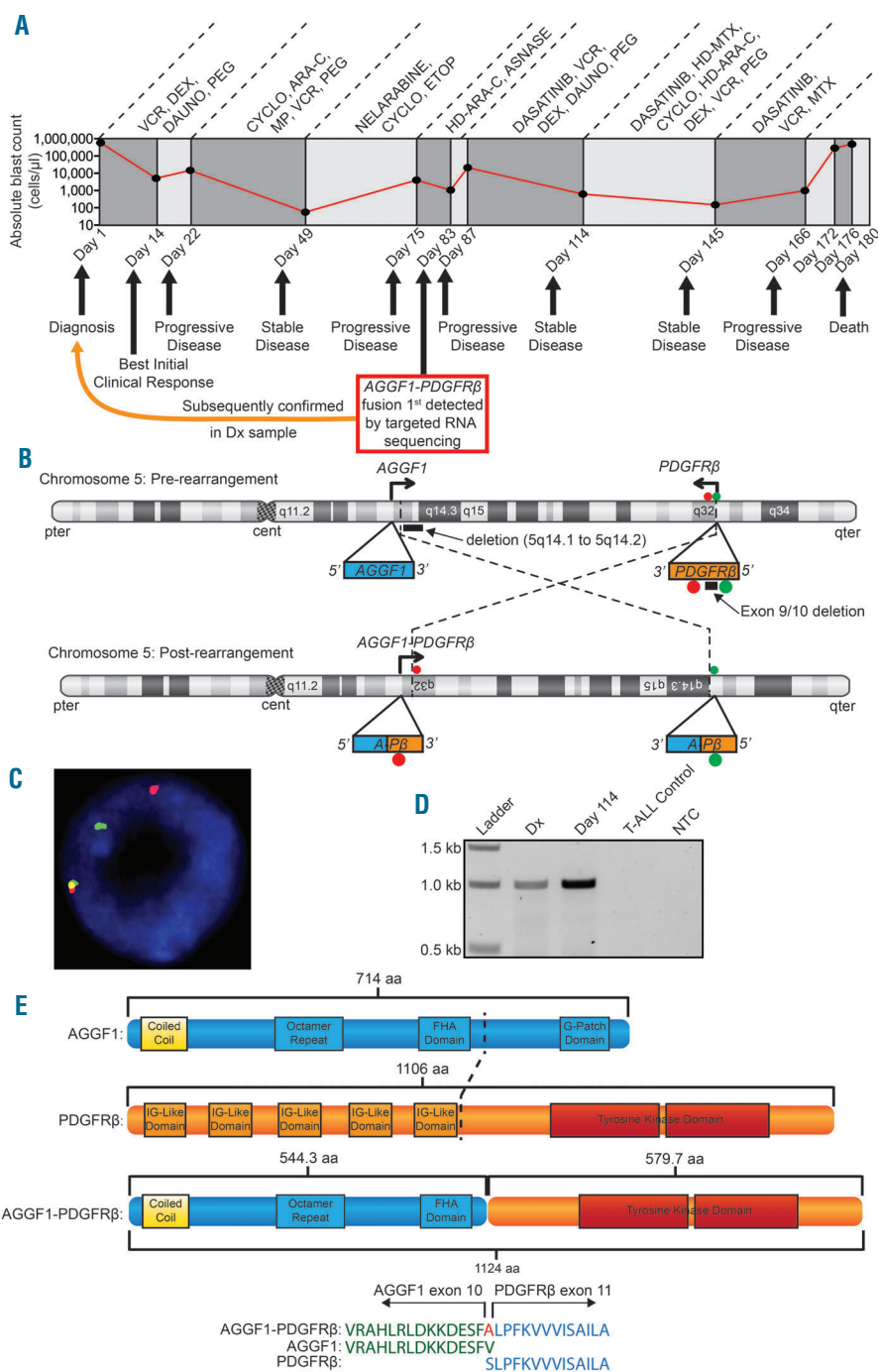


Figure 1. Characterization of a novel *AGGF1-PDGFRβ* fusion identified in a pediatric T-ALL patient. (A) Clinical timeline of the patient's treatment history from diagnosis until death. Treatment at various timepoints is shown along the top of the timeline, clinical response is indicated along the bottom, and absolute blast count (cells/ μ L) is indicated by the red line. The *AGGF1-PDGFRβ* fusion gene was first detected in a sample obtained on day 83, and its presence subsequently confirmed in the diagnostic sample. VCR, vincristine; DEX, dexamethasone; DAUNO, daunorubicin; PEG, pegaspargase; CYCLO, cyclophosphamide; ARA-C, cytarabine; MP, mercaptopurine; ETOP, etoposide; HD, high dose; ASNASE, asparaginase; MTX, methotrexate. Intrathecal chemotherapy was also delivered throughout each treatment phase. (B) A schematic representation of the paracentric 5q inversion resulting in the *AGGF1-PDGFRβ* fusion. The top schematic shows an unaltered chromosome 5, and the bottom schematic shows the result of the rearrangement (pter, telomeric region of the short arm; qter, telomeric region of the long arm; cent, centromeric region). The *AGGF1* and *PDGFRβ* loci are shown with arrows indicating the direction of transcription. The red and green dots under the *PDGFRβ* locus represent the FISH probes. The black rectangles indicate the locations of a 4.6 Mb deletion (5q14.1 to 5q14.2) and a 2.5 kb deletion involving exons 9 and 10 of *PDGFRβ* (not drawn to scale). The dashed lines represent the inversion breakpoints and the inversion. This rearrangement splits the *PDGFRβ* probes, and causes the *AGGF1-PDGFRβ* fusion. (C) FISH was performed on cells in interphase using the *PDGFRβ* Break Apart probe (Abbott Molecular, Des Plaines, IL, USA) according to the manufacturer's recommendations. Images were captured by an Olympus BX41TF microscope equipped with a Jenoptik camera and analyzed with Isis Software (MetaSystems). (D) Polymerase chain reaction amplification across the *AGGF1-PDGFRβ* fusion gene breakpoint in primary patient's specimens. An ~1 kb product (predicted product size: 1.001 kb) was amplified from diagnostic (Dx; day 1) and longitudinal (day 114) specimens using primers AGGF1_1152_F and PDGFRβ_2153_R (see *Online Supplementary Table S1*). Additional lanes include a no template control (NTC) and a reaction in which the input cDNA came from a pediatric T-ALL specimen that does not involve an *AGGF1-PDGFRβ* fusion kinase. The N-terminal component consists of *AGGF1* exons 1-10 encoding 544 amino acid residues, including a coiled coil domain that controls homodimerization of the fusion kinase. After an intervening alanine residue at the *AGGF1/PDGFRβ* junction, the C-terminal component consists of *PDGFRβ* exons 11-23 encoding 579 amino acid residues and retaining the entire split tyrosine kinase domain.

2F). Incubation of Ba/F3 AGGF1-PDGFR β cells with PDGFR β tyrosine kinase inhibitors caused concentration-dependent inhibition of AGGF1-PDGFR β autophosphorylation, as evidenced by decreased PDGFR β ^{Y751} phosphorylation (Figure 2G).

Given its clinical activity in PDGFR β -driven malignancies and Philadelphia (Ph) chromosome-positive ALL, dasatinib was added to the patient's treatment regimen in combination with cycles of multiagent chemotherapy (Figure 1A, *Online Supplementary Table S1*). This therapy

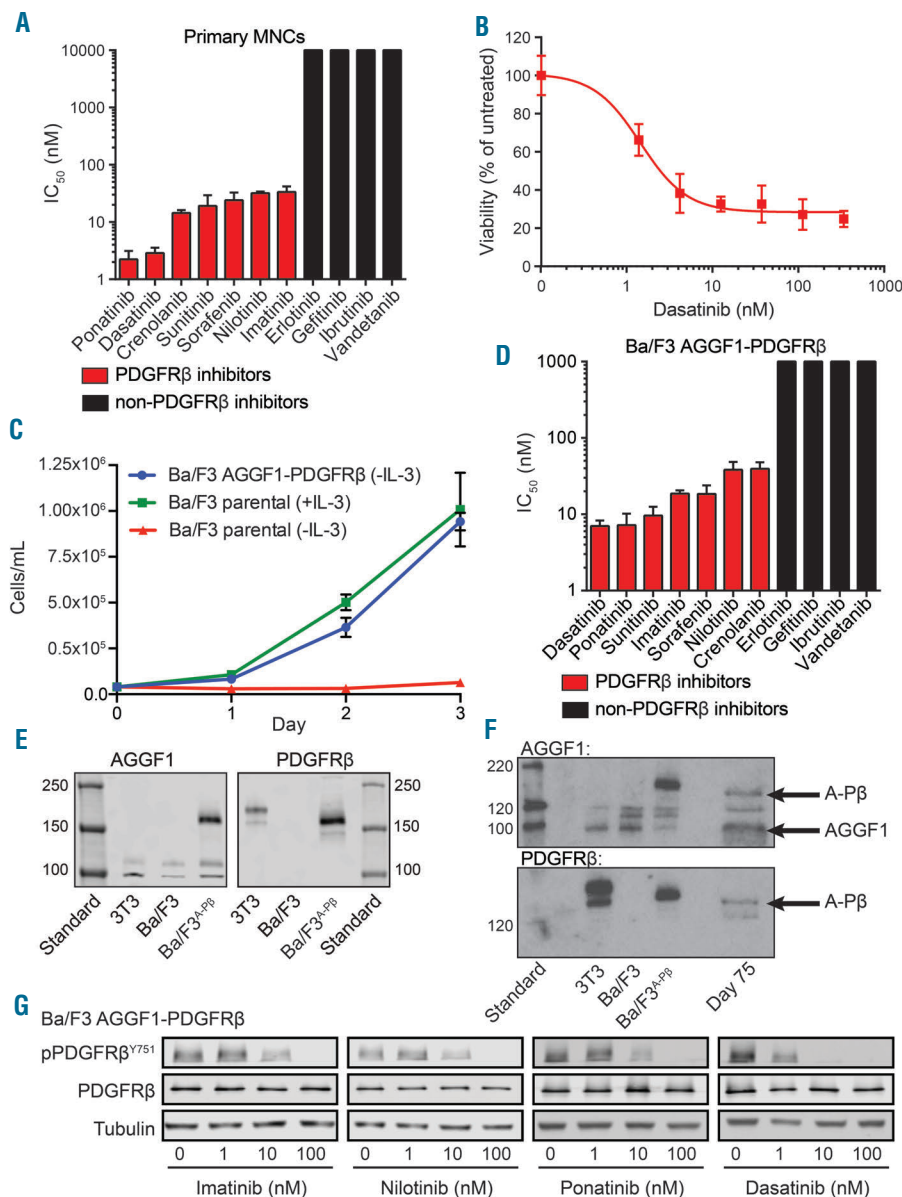


Figure 2. Inhibitor sensitivity profiling and transformation capacity of cells expressing the AGGF1-PDGFR β fusion kinase. (A) *Ex vivo* response of primary mononuclear cells (MNCs) from the pediatric AGGF1-PDGFR β -positive T-ALL patient to tyrosine kinase inhibitors with targeting profiles that include (red bars) or do not include PDGFR β (black bars). Mononuclear cells isolated from whole blood were distributed in 384-well plates and subjected to graded concentrations of tyrosine kinase inhibitors. Viability was assessed after 72 h via a methanethiosulfonate (MTS)-based viability assay (CellTiter 96 Aqueous One), from which IC₅₀ values (shown as the mean of three replicates \pm SEM) were calculated. (B) *Ex vivo* dose-response sensitivity of primary mononuclear cells from this patient to dasatinib. (C) Comparative outgrowth of Ba/F3 AGGF1-PDGFR β cells and parental Ba/F3 cells upon withdrawal of interleukin-3 (IL-3). Ba/F3 cells cultured in the presence or absence of 10% WEHI-conditioned medium as a source of IL-3 were included as a control. The AGGF1-PDGFR β fusion gene was cloned into pMSCV-IRES-GFP (In-Fusion cloning kit; Clontech) and used to infect murine Ba/F3 cells. The fusion kinase was shown to be transforming by its ability to confer IL-3 independence on Ba/F3 cells. (D) Response of Ba/F3 AGGF1-PDGFR β cells to the same panel of tyrosine kinase inhibitors as in (A). (E) NIH 3T3 cells, parental Ba/F3 cells and Ba/F3 AGGF1-PDGFR β cells (Ba/F3^{AGGF1}) were pelleted, lysed in RIPA buffer, quantitated, then boiled for 10 min in SDS-polyacrylamide gel electrophoresis loading buffer. Equal amounts of lysates were separated on 4–15% Tris-glycine gels, transferred and immunoblotted for AGGF1 (Abnova #PAB28125) and PDGFR β [Cell Signaling Technology (CST) #3169]. (F) Lysates of NIH 3T3 cells, parental Ba/F3 cells, Ba/F3 AGGF1-PDGFR β cells, and patient-derived blasts sorted from the day 75 specimen were prepared as above, separated on 4–15% Tris-glycine gels, transferred and immunoblotted for AGGF1 (Abnova #PAB28125). (G) Immunoblot analysis of lysates from Ba/F3 AGGF1-PDGFR β cells treated with graded concentrations of clinically approved tyrosine kinase inhibitors that target PDGFR β . Following 4 h of exposure to tyrosine kinase inhibitors, lysates were prepared as described above and immunoblotted for total PDGFR β (CST #3169), phospho-PDGFR β ^{Y751} (CST #4549), and tubulin (CST #2148).

was well tolerated and the patient had stabilization of disease with an improvement in splenomegaly and clinical symptoms that lasted for 3 months. His disease, however, rapidly progressed after this time and he expired 6 months after diagnosis.

The only reported *AGGF1*-containing fusion is *AGGF1-RAF1*, observed in papillary thyroid carcinoma and prostate cancer.⁴ *PDGFRβ*-containing fusions have been reported in B-cell malignancies,^{5,6} but not T-ALL. Fusions of the B-cell lymphoid transcription factor early B-cell factor 1 (*EBF1*) with *PDGFRβ* occur in ~8% of children with Ph-like ALL.⁷ The breakpoint of *PDGFRβ* (L528, *PDGFRβ* numbering) is conserved between our *AGGF1-PDGFRβ* T-ALL case, *EBF1-PDGFRβ* B-ALL cases⁷ and *NDEL1-PDGFRβ* in a myeloid malignancy with eosinophilia.⁸

Following the paradigm of combining a tyrosine kinase inhibitor with chemotherapy for treatment of pediatric Ph-positive ALL,⁹ reports of favorable responses to tyrosine kinase inhibitor therapy in cases of Ph-like ALL^{7,10} provided the rationale for our treatment approach. Patients with chronic myeloid malignancies harboring *PDGFRβ* fusions achieve durable remissions with imatinib.^{5,11} Imatinib and dasatinib have been safely combined with multiagent chemotherapy in children with Ph+ ALL^{9,12} and both drugs demonstrated activity against this patient's blasts *ex vivo*. We used dasatinib because the patient had concomitant central nervous system leukemia and dasatinib has superior penetration into the central nervous system.¹³ While this patient ultimately failed to achieve a durable response to a dasatinib-containing regimen, he experienced disease stabilization for 3 months after dasatinib was added to conventional chemotherapy. The relapse suggests additional genetic alterations were present and/or the *AGGF1-PDGFRβ* fusion was limited to a major subclone.

Ph-like ALL is a recently described subtype of leukemia characterized by genetic alterations that deregulate cytokine receptor and tyrosine kinase signaling,¹² including ABL-class rearrangements that encode fusion genes involving *ABL1*, *ABL2*, *CSF1R* and *PDGFRβ*. Ph-like ALL is typically observed in B-ALL. Translocation and overexpression of the transcription factors *TLX1* and *TLX3* have been associated with ABL class fusions in a subset of T-ALL. RNA-seq analysis on the T-ALL patient's day 75 specimen revealed no alterations in these *TLX* family members. Rather, we observed striking overexpression of the T-cell transcription factors, *TAL1* and *LYL1* (Online Supplementary Table S4). Coordinated overexpression of *TAL1* and *LYL1* has been observed previously in T-ALL specimens,^{14,15} suggesting a possible oncogenic role. Liu *et al.* reported a clustering analysis from 264 pediatric T-ALL specimens based on dysregulated transcription factor expression as well as hierarchical clustering of RNA-seq gene expression data.¹⁵ We compared our T-ALL patient's day 75 specimen RNA-seq data on 19 transcription factors to the 264 specimens reported by Liu *et al.*¹⁵ and found that this specimen clustered most closely with *TAL1*/*LYL1* specimens within the *TAL1* subgroup (Online Supplementary Figure S4). Two control cell lines [ALL-SIL (*TLX1*); HPB-ALL (*TLX3*)] clustered in their expected subgroups. We have presented the first reported case of Ph-like ALL with a *PDGFRβ* rearrangement in a child with T-lineage disease and highlight the role of aberrant, therapeutically targetable kinase signaling in a subset of childhood ALL that spans all lineages.

Matthew S. Zabriskie,¹ Orlando Antelope,¹ Anupam R. Verma,² Lauren R. Draper,³ Christopher A. Eide,^{3,4} Anthony D.

Pomicer,¹ Thai Hoa Tran,⁵ Brian J. Druker,^{3,4} Jeffrey W. Tyner,³ Rodney R. Miles,^{1,6} James M. Graham,^{1,7} Jae-Yeon Hwang,^{1,7} Katherine E. Varley,^{1,7} Reha M. Toydemir,^{6,8} Michael W. Deininger,^{1,9} Elizabeth A. Raetz^{1,2,5} and Thomas O'Hare^{1,2,5}

¹Huntsman Cancer Institute, University of Utah, Salt Lake City, UT; ²Department of Pediatrics, Division of Pediatric Hematology/Oncology, University of Utah, Salt Lake City, UT; ³Knight Cancer Institute, Oregon Health & Science University, Portland, OR; ⁴Howard Hughes Medical Institute, Portland, OR; ⁵Helen Diller Family Cancer Research Center, Benioff Children's Hospital, San Francisco, CA; ⁶Department of Pathology, University of Utah, Salt Lake City, UT; ⁷Department of Oncological Sciences, University of Utah, Salt Lake City, UT; ⁸Department of Pediatrics, Division of Medical Genetics, University of Utah, Salt Lake City, UT and ⁹Division of Hematology and Hematologic Malignancies, University of Utah, Salt Lake City, UT, USA

*MSZ and OA contributed equally. ⁵EAR and TO contributed equally

Acknowledgments: we acknowledge the Pediatric Cancer Program Biobank with support from the Primary Children's Hospital and Intermountain Healthcare Foundations and the Children's Oncology Group Cell Bank. We acknowledge Amber D. Bowler for technical assistance.

Funding: research reported in this publication was supported by the National Cancer Institute (NCI) of the National Institutes of Health (NIH) under Award Number R01CA178397. The authors acknowledge support of funds in conjunction with the NIH / NCI Cancer Center Support Grant P30CA042014 awarded to the Huntsman Cancer Institute. JWT was supported by The Leukemia & Lymphoma Society, the V Foundation for Cancer Research, the Gabrielle's Angel Foundation for Cancer Research, and the NCI (5R00CA151457-04; 1R01CA183947-01). BJD is an investigator for the Howard Hughes Medical Institute and is also supported by the NCI (2R01CA065823-21A1). JWT receives research support from Aptose, Array, AstraZeneca, Constellation, Genentech, Gilead, Incyte, Janssen, Seattle Genetics, Syros, Takeda; Scientific Advisory Board for Leap Oncology. B.J.D.'s institution (OHSU) receives clinical trial funding from Novartis, Bristol-Myers Squibb, and ARIAD.

Correspondence: Thomas.OHare@hci.utah.edu or Elizabeth.Raetz@hci.utah.edu
doi:10.3324/haematol.2017.165282

Information on authorship, contributions, and financial & other disclosures was provided by the authors and is available with the online version of this article at www.haematologica.org.

References

- Moricke A, Zimmermann M, Valsecchi MG, et al. Dexamethasone vs prednisone in induction treatment of pediatric ALL: results of the randomized trial AIEOP-BFM ALL 2000. *Blood*. 2016;127(17):2101-2112.
- Reismuller B, Attarbaschi A, Peters C, et al. Long-term outcome of initially homogeneously treated and relapsed childhood acute lymphoblastic leukaemia in Austria—a population-based report of the Austrian Berlin-Frankfurt-Munster (BFM) Study Group. *Br J Haematol*. 2009;144(4):559-570.
- Tyner JW, Yang WF, Bankhead A, 3rd, et al. Kinase pathway dependence in primary human leukemias determined by rapid inhibitor screening. *Cancer Res*. 2013;73(1):285-296.
- Stransky N, Cerami E, Schalm S, Kim JL, Lengauer C. The landscape of kinase fusions in cancer. *Nat Commun*. 2014;5:4846.
- Cheah CY, Burbury K, Apperley JF, et al. Patients with myeloid malignancies bearing *PDGFRβ* fusion genes achieve durable long-term remissions with imatinib. *Blood*. 2014;123(23):3574-3577.
- Schwab C, Ryan SL, Chilton L, et al. *EBF1-PDGFRβ* fusion in pediatric B-cell precursor acute lymphoblastic leukemia (BCP-ALL): genetic profile and clinical implications. *Blood*. 2016;127(18):2214-2218.
- Roberts KG, Li Y, Payne-Turner D, et al. Targetable kinase-activating lesions in Ph-like acute lymphoblastic leukemia. *N Engl J Med*. 2014;371(11):1005-1015.

8. Byrgazov K, Goma M, Hoermann G, et al. NDEL1-PDGFRB fusion gene in a myeloid malignancy with eosinophilia associated with resistance to tyrosine kinase inhibitors. *Leukemia*. 2017;31(1):237-240.
9. Schultz KR, Carroll A, Heerema NA, et al. Long-term follow-up of imatinib in pediatric Philadelphia chromosome-positive acute lymphoblastic leukemia: Children's Oncology Group study AALL0031. *Leukemia*. 2014;28(7):1467-1471.
10. Lengline E, Beldjord K, Dombret H, Soulier J, Boissel N, Clappier E. Successful tyrosine kinase inhibitor therapy in a refractory B-cell precursor acute lymphoblastic leukemia with EBF1-PDGFRB fusion. *Haematologica*. 2013;98(11):e146-148.
11. Apperley JF, Gardembas M, Melo JV, et al. Response to imatinib mesylate in patients with chronic myeloproliferative diseases with rearrangements of the platelet-derived growth factor receptor beta. *N Engl J Med*. 2002;347(7):481-487.
12. Slayton WB, Schultz KR, Jones T, et al. Continuous dose dasatinib is safe and feasible in combination with intensive chemotherapy in pediatric Philadelphia chromosome positive acute lymphoblastic leukemia (Ph+ ALL): Children's Oncology Group (COG) trial AALL0622. *Blood*. 2012;120(21):137.
13. Porkka K, Koskenvesa P, Lundan T, et al. Dasatinib crosses the blood-brain barrier and is an efficient therapy for central nervous system Philadelphia chromosome-positive leukemia. *Blood*. 2008;112(4):1005-1012.
14. Ferrando AA, Neuberg DS, Staunton J, et al. Gene expression signatures define novel oncogenic pathways in T cell acute lymphoblastic leukemia. *Cancer Cell*. 2002;1(1):75-87.
15. Liu Y, Easton J, Shao Y, et al. The genomic landscape of pediatric and young adult T-lineage acute lymphoblastic leukemia. *Nat Genet*. 2017;49(8):1211-1218.